

SrAl₄O₇:Tm³⁺/Yb³⁺ nanocrystalline blue phosphor: structural, thermal and optical properties

N.K. Giri · S.K. Singh · D.K. Rai · S.B. Rai

Received: 31 August 2009 / Revised version: 23 November 2009 / Published online: 14 January 2010
© Springer-Verlag 2010

Abstract Strontium aluminate (SrAl₄O₇) nanophosphor codoped with Tm³⁺–Yb³⁺ has been synthesized through the combustion route using urea as the reducing agent. Structural, thermal and optical characterizations have been carried out. Heat treatment of the samples shows a change in the crystallite phases and the relative luminescence intensities for the different bands. The nanocrystalline particles in the as-synthesized sample seem to arrange in rod like shapes of submicrometer length on annealing. A broad (350–550 nm) emission in the UV–green region is observed when 266 nm radiation is used for excitation. Intense upconversion (UC) emissions in blue, red and infrared are seen with excitation by 976 nm radiation. An emission at 364 nm not observed earlier and attributed to $^1\text{D}_2 \rightarrow ^3\text{H}_6$ transition in Tm³⁺ is also seen. The blue emission from SrAl₄O₇:Tm³⁺/Yb³⁺ codoped nanophosphor (annealed at 1200°C) exhibits high color purity (89%) and is comparable to phosphors used commercially. The energy transfer mechanisms, responsible for these UC emissions, are proposed and discussed.

1 Introduction

Studies of materials in nanosize are being extensively studied as they show significantly changed properties as compared to their bulk counterpart [1]. Such materials especially inorganic nanocrystal are prepared by a variety of methods [2–7] of which the solution combustion technique [7] not

only is a simple and low cost method resulting in homogeneous materials but also permits doping with rare earths in a single step [8, 9]. These nanocrystallites doped with rare earth ions yield many upconverted emission bands when excited with NIR diode laser. In case the intermediate excited state is long lived the efficiency is greatly increased. This permits oxide based phosphor materials which are easily processed and have greater stability to be used in place of sulphide based phosphors [10–15].

The use of a red emitting laser as excitation source for a Tm³⁺ doped inorganic nanophosphors gives emission in the blue region [16]. In order to obviate the use of the red emitting laser and use instead a laser emitting in the NIR, the nanocrystallite has to be doped with an additional rare earth absorbing the NIR radiation and transferring its excitation energy to the Tm³⁺ ion. Yb³⁺ ion, absorbing at 976 nm, is such an ion [17].

In the present work strontium aluminate (SrO–Al₂O₃) has been investigated as a host for Tm³⁺ and for Tm³⁺, Yb³ together. This SrO–Al₂O₃ can exist in several phases SrAl₂O₄, SrAl₁₂O₁₉, Sr₂Al₆O₁₁, and Sr₄Al₁₄O₂₅ [18–20]. The SrAl₄O₇ (SAL) phase after doping with lanthanide ions is not yet well characterized though it is of great interest as it has a long-duration persistence luminescence [21]. Its blue emission is used as a biological marker [22] and an efficient high resolution display phosphor [23]. Its synthesis, structural characterization and luminescence are discussed in the present note.

2 Experimental

The strontium aluminate phosphor samples were synthesized through the combustion route using urea as an organic

N.K. Giri · S.K. Singh · D.K. Rai · S.B. Rai (✉)
Laser and Spectroscopy Laboratory, Department of Physics,
BHU, Varanasi 05, India
e-mail: sbrai49@yahoo.co.in
Fax: +91-542-2369889

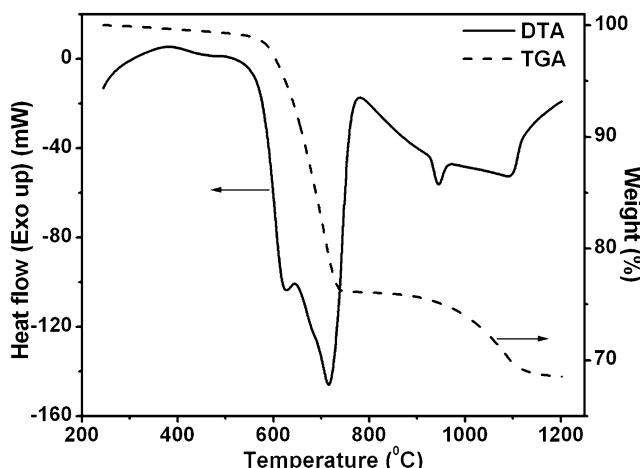


Fig. 1 Differential thermal analysis (DTA) and thermogravimetric analysis (TGA) curves of the as-synthesized phosphor sample

fuel. A detail of the preparation method is as described earlier [24]. The starting composition of the material is



where $x = 1.0, 2.0 \text{ mol\%}$ and $y = 0.5, 1.0 \text{ mol\%}$.

The differential thermal analysis (DTA) and thermogravimetric analysis (TGA) of the sample have been carried out in a nitrogen atmosphere on a Pyris Diamond thermal analyzer EXSTAR 6000 unit (Perkin Elmer). The as-synthesized samples were annealed at two different temperatures 800°C and 1200°C for 10 h. X-ray diffraction (XRD) patterns have been recorded using a 18 kW rotating anode (Cu) based Regaku powder diffractometer fitted with a graphite monochromator. The degree of crystallization and the size of the crystallites are estimated from these studies. Transmission electron microscope (TEM) image of the sample has been recorded using a Technai 20G², Philips unit. Fourier transform infrared (FTIR) spectra of three types of samples have been recorded using a Spectrum RX-I spectrophotometer (Perkin Elmer). The absorption spectrum of the sample was recorded in the reflectance mode (as the sample is opaque) using Perkin Elmer, Lambda-35 spectrophotometer.

The downconversion spectra are recorded after excitation of the sample with 266 nm radiation from a Nd:YAG laser (Innolas, Spitlight 600, 7 ns pulse width) using a fluorescence spectrometer (QE 65000, Ocean Optics, USA). The upconversion (UC) luminescence measurements are carried out by exciting the samples with the 976 nm radiation from a diode laser and recorded on iHR320, Horiba Jobin Yvon, spectrometer.

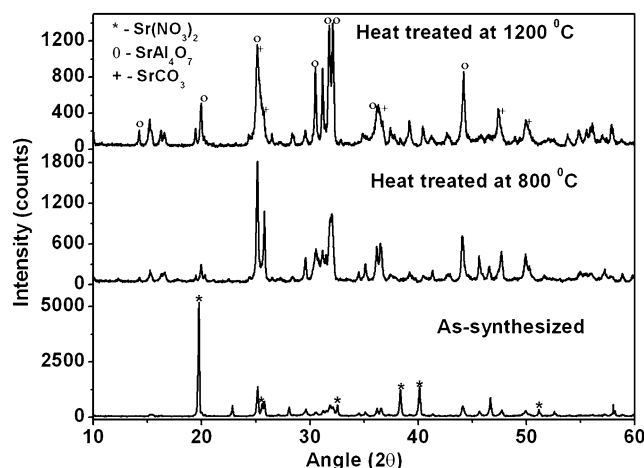


Fig. 2 X-ray diffraction (XRD) patterns of $\text{SrAl}_4\text{O}_7: \text{Tm}^{3+} + \text{Yb}^{3+}$ phosphor as-synthesized, heat treated at 800°C and at 1200°C

3 Results and discussion

3.1 Thermal analysis

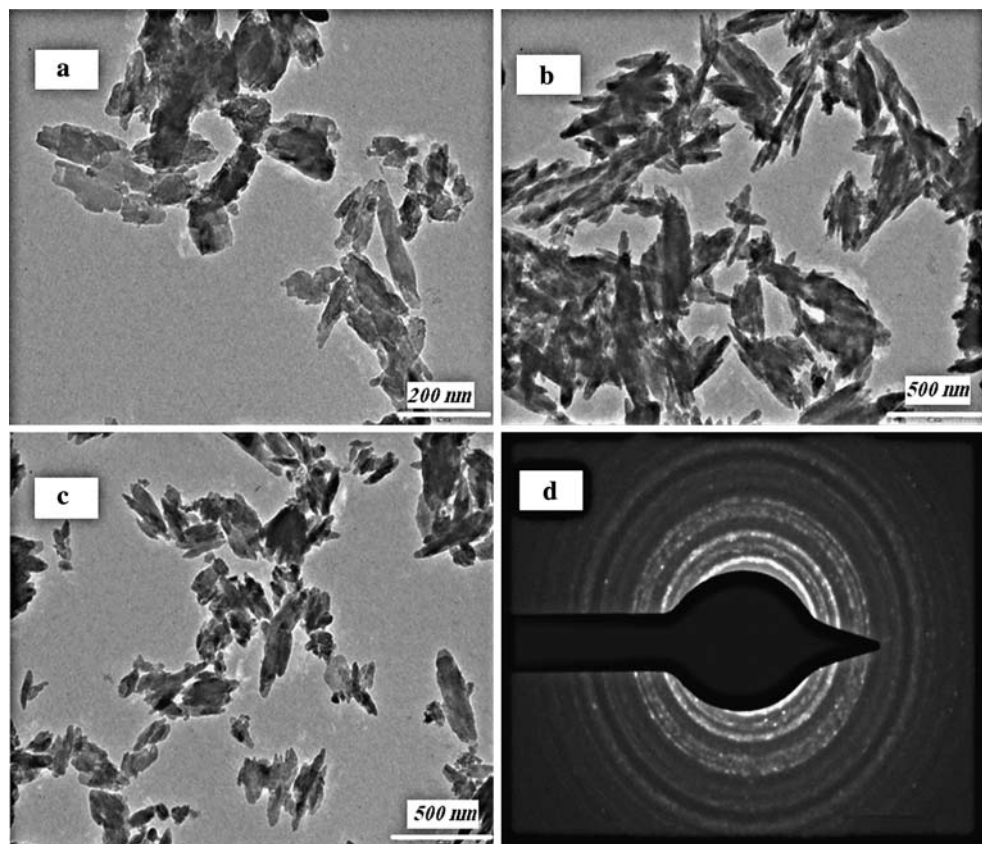
In DTA, any change in the sample results in heat absorption or heat emission (measured as change in power and measured in mW) relative to a reference material on the other hand TGA detects any change in weight. Figure 1 shows the DTA and TGA curves for an as-synthesized phosphor material. The TGA curve shows a weight loss of about 25% between 550 – 750°C associated with two endothermic peaks, one at 620°C and the other at 710°C , as evident from the DTA curve. This weight loss may be attributed to the conversion of the nitrates (starting material for synthesis) into oxide and the loss of the volatile components. A small weight loss of about ten percent is also seen and is associated with the endothermic peaks seen at 945°C and at 1100°C . This is due to the decomposition of the strontium carbonate (SrCO_3) [25]. Thus, thermal analysis suggests that the change takes place in two steps: first near 700°C and the second near 1100°C . This makes it essential to study three samples: one as-synthesized, the second heated at 800°C and the third heated to 1200°C . Samples were kept at these temperatures for 10 h.

3.2 Structural features and analysis

3.2.1 X-ray diffraction (XRD)

The X-ray diffraction patterns of all the three types of the sample, one ‘as-synthesized’ and the other two obtained after the different temperatures are shown in Fig. 2. The presence of sharp and intense diffraction peaks indicate the crystalline nature of the phosphor material. Peaks due to SrAl_4O_7 , $\text{Sr}(\text{NO}_3)_2$ and SrCO_3 are seen in the XRD pattern of the as-synthesized sample. The sample heat treated

Fig. 3 Transmission electron micrographs (TEM) along with the selected area electron diffraction (SAED) pattern of the SrAl₄O₇:Tm³⁺ + Yb³⁺ phosphor sample annealed at 1200°C. Micrographs (a), (b) and (c) show the presence of the micron-size rod like structure while sharp rings in SAED pattern (d) shows the crystalline nature



at 800°C has peaks due only to SrAl₄O₇ and to SrCO₃. The peaks due to SAL are more pronounced. For the sample heated to 1200°C the peak due to SrCO₃ becomes almost insignificant. Zhang et al. [26] have also reported similar results.

3.2.2 Transmission electron microscopy (TEM)

The TEM picture for the ‘as-synthesized’ sample indicates that the phosphor material contains highly agglomerated nanocrystals of an average crystal size of ~54 nm. For the sample heated at 1200°C the agglomerated nanocrystals form a rod like structure of submicrometer length and width ~60 nm. Figure 3 shows the TEM images (a, b, c) along with selected area electron diffraction (SAED) pattern (d) for a Tm³⁺-Yb³⁺ codoped sample heated at 1200°C for 10 h. It is likely that it is the heat treatment which leads to the formation of rod like structure. The bright rings seen are indicative of the crystalline nature of the sample.

3.3 Optical characterization

3.3.1 Fourier transform infrared (FTIR) analysis

The FTIR spectra of the three Tm³⁺-Yb³⁺ doped phosphor samples in the 4000–400 cm⁻¹ region (Fig. 4) show nearly

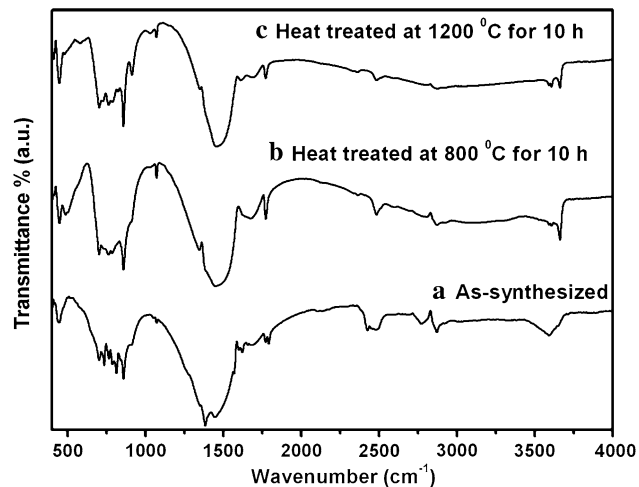


Fig. 4 Fourier transform infrared (FTIR) spectra of SrAl₄O₇:Tm³⁺ + Yb³⁺ nanophosphor samples (a) as-synthesized, (b) heat treated at 800 °C and (c) heat treated at 1200 °C (all the samples have been heat treated for 10 h)

similar spectrum. The spectrum shows a doublet structure near 445 cm⁻¹ and a broad absorption containing several vibrational peaks in 700–900 cm⁻¹ region. The doublet at 445 cm⁻¹ is due to the bending vibration of the O-Al-O bonds [27]. The peaks in the 700–900 cm⁻¹ region are attributed to the metal oxygen bonds in the SrAl₄O₇ struc-

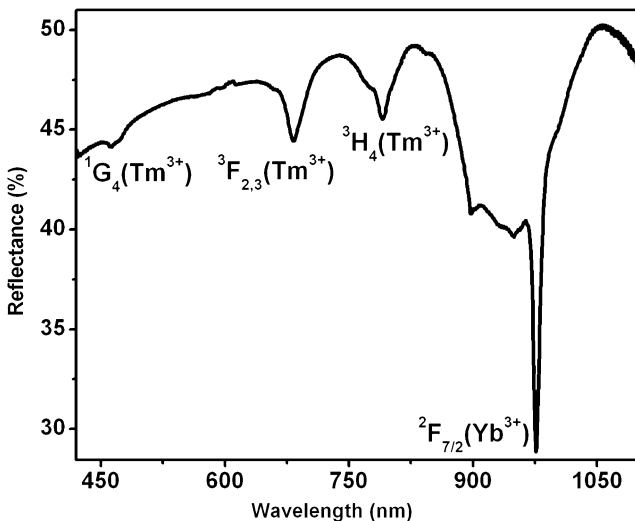


Fig. 5 The absorption spectrum of nanocrystalline strontium aluminate nanophosphor doped with Tm^{3+} (0.5 mol%) and Yb^{3+} (2.0 mol%) annealed at 1200°C in reflectance mode

ture [28]. The sharp absorption band near 1070 cm^{-1} corresponds to the Al–O stretching vibration [29]. Peaks in the region 1340 – 1780 cm^{-1} exhibit the typical features of “nitrate (NO_3^-)” and “ CO_3^{2-} anion” vibrations. The strong band at 1450 cm^{-1} is associated with the carbonyl ions and becomes weak as the annealing temperature is increased. The broad band near 3600 cm^{-1} is due to (O–H) stretching in the adsorbed water. On heat treatment at high temperatures such bands become very weak or are not seen.

3.3.2 Absorption spectrum

The absorption spectrum of the strontium aluminate nanophosphor doped with Tm^{3+} (0.5 mol%) and Yb^{3+} (2.0 mol%) and heated at 1200°C for 10 h in the reflectance mode is shown in Fig. 5. The five absorption peaks at 467, 660, 681, 790 and 976 nm are assigned to the $^3\text{H}_6 \rightarrow ^1\text{G}_4$, $^3\text{H}_6 \rightarrow ^3\text{F}_3$, $^3\text{H}_6 \rightarrow ^3\text{F}_2$, $^3\text{H}_6 \rightarrow ^3\text{H}_4$ transitions in Tm^{3+} and to the $^2\text{F}_{7/2} \rightarrow ^2\text{F}_{5/2}$ transition in Yb^{3+} , respectively.

3.3.3 Luminescence excited by 266 nm laser radiation

The room temperature emission spectrum of the nanocrystalline SrAl₄O₇:Tm³⁺/Yb³⁺ and SrAl₄O₇:Tm³⁺ systems annealed at 1200°C on excitation with 266 nm radiation is shown in Fig. 6. The incident radiation excites the Tm³⁺ ions to the ³P manifold resulting in a number of luminescence bands. For both samples a broad emission is seen (between 350–550 nm) with three intense peaks at 390 nm (¹I₆ → ³H₅), 464 nm (¹D₂ → ³F₄) and 479 nm (¹G₄ → ³H₆) due to Tm³⁺ excitation superposed. The ¹I₆ → ³H₅ peak at 390 nm is weaker in the Tm³⁺-Yb³⁺ codoped sample while the ¹D₂ → ³F₄ peak at 464 nm becomes very broad. The

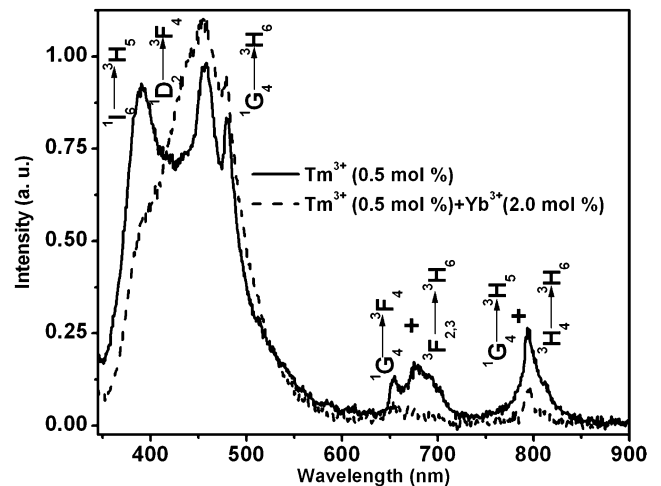


Fig. 6 Room temperature downconversion spectrum (350–900 nm) of nanocrystalline $\text{SrAl}_4\text{O}_7:\text{Tm}^{3+}$ and $\text{Tm}^{3+} + \text{Yb}^{3+}$ nanophosphor (heat treated at 1200°C for 10 h) on excitation with 266 nm

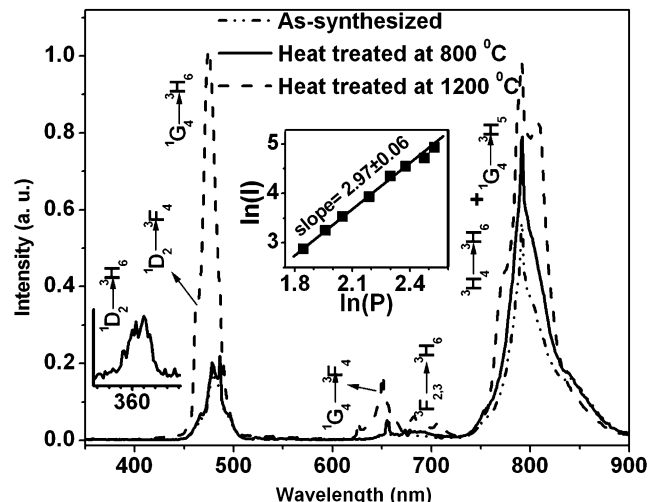


Fig. 7 Upconversion spectrum ($\lambda_{\text{ex}} = 976$ nm) of SrAl_4O_7 : Tm^{3+} + Yb^{3+} nanophosphor **(a)** as-synthesized, **(b)** heat treated at 800°C and **(c)** heat treated at 1200°C for 10 h. A power dependence plot for blue emission is shown in the *inset* (slope = 2.97 ± 0.06). An enlarged emission at 364 nm is shown at the *bottom* of the figure

emission in the red region between 640–720 nm corresponding to the ${}^1G_4 \rightarrow {}^3F_4 / {}^3F_{2,3} \rightarrow {}^3H_6$ transitions in Tm $^{3+}$ also becomes much weaker in the codoped samples. The broad emission in the near infrared (NIR) region (760–850 nm) assigned to the ${}^1G_4 \rightarrow {}^3H_5 / {}^3H_4 \rightarrow {}^3H_6$ transitions in Tm $^{3+}$ also has its intensity reduced considerably in the codoped sample. To conclude, the addition of Yb $^{3+}$ to the strontium aluminate containing Tm $^{3+}$ reduces the intensity of the luminescence in red and NIR regions of the spectrum.

This reduction in intensity indicates that some excitation energy is being transferred from Tm^{3+} (3H_4) to Yb^{3+} ($^2F_{5/2}$). Energy transfer from Tm^{3+} (3H_4) to Yb^{3+} ($^2F_{5/2}$)

has been reported by Pandozzi et al. [30] in Gd₃Ga₅O₁₂: Tm³⁺/Yb³⁺ nanocrystals.

3.3.4 Upconversion luminescence on 976 nm excitation

Phosphor sample containing only Tm³⁺ does not show any luminescence when irradiated with 976 nm radiation, but a sample with both Tm³⁺ and Yb³⁺ shows luminescent emission from Tm³⁺. Figure 7 shows the room temperature luminescence from a strontium aluminate phosphors containing Tm³⁺ (0.5 mol%) + Yb³⁺ (2.0 mol%) and annealed at two different temperatures for the same duration (10 h). It is seen that the luminescence intensity is higher for the sample annealed at higher temperature. This increase in intensity is to be ascribed to the removal of the fluorescence quenching centers, e.g. O–H. Though the increase in the intensity of all the UC emissions takes place it is relatively very high for the blue emission.

The incident radiation is absorbed by Yb³⁺ ions exciting these to ²F_{5/2} level. The excitation energy can be and possibly is transferred to Tm³⁺ ions. Two alternative pathways are possible for the excitation of the Tm³⁺ ions to the ¹G₄ state from which many of the observed luminescence bands arise. These are

- (i) ${}^2F_{5/2}(\text{Yb}^{3+})$, ${}^3H_6(\text{Tm}^{3+}) \rightarrow {}^2F_{7/2}(\text{Yb}^{3+})$, ${}^3H_5(\text{Tm}^{3+})$ and
- (ii) $2({}^2F_{5/2} \rightarrow {}^2F_{7/2}) \text{ Yb}^{3+} \rightarrow ({}^3H_6 \rightarrow {}^1G_4) \text{ Tm}^{3+}$

Equation (i) depicts the first step in the first pathway known as the sequential sensitization process. It is obvious that this step involves a non-resonant process and so is not a very likely process. However, once Tm³⁺ is excited to the ³H₅ state a non-radiative relaxation brings it to relatively long lived ³F₄ state. Tm³⁺ ions in this ³F₄ state can absorb a second 976 nm photon getting excited to the ³F₂ level. Tm³⁺ ions in this ³F₂ state again relax non-radiatively via ³F₃ to the ³H₄ level and a third 976 nm photon excites such ions to the ¹G₄ level. Thus in the first pathway for energy transfer from Yb³⁺ to Tm³⁺ one requires three photons to excite the latter (Tm³⁺) ion to the ¹G₄ level (Fig. 8). The non-resonant character of the different steps is taken care of by the vibrations in the host lattice. The UC spectrum is shown in Fig. 7. The ¹D₂ level having an excitation energy greater than ¹G₄ is populated by absorption of the photon emitted (by Tm³⁺) in the transition ¹G₄ → ³F₄ by ions in the ³H₄ level. Additional excitation of ions to the ¹D₂ state can occur by the absorption of a photon emitted in the transition ³H₄ → ³F₄ (Tm³⁺) by Tm³⁺ ions in ¹G₄ state.

The second pathway of energy transfer from Yb³⁺ ions to Tm³⁺ ions called the cooperative sensitization, involves the simultaneous transfer of total excitation energy of Yb³⁺ ion pair in the excited ²F_{5/2} level to a Tm³⁺ ion. The Tm³⁺ ions is thereby directly excited to the ¹G₄ state, so that only

two incident photons are required to excite Tm³⁺ ion to the ¹G₄ state. The intensity of the blue emission (at 479 nm) as a function of incident laser power is plotted in a log $I - \log P$ plot. The straight line has a slope of ~3 (2.97 ± 0.06) thereby indicating that three incident photons are involved in the excitation of the ¹G₄ level. Since the concentration of Yb³⁺ ions in the present sample is only two mol% it is not surprising that the cooperative energy transfer from a pair of excited Yb³⁺ ions does not make a larger contribution to the observed luminescence. The ultraviolet upconverted emission at 364 nm and the blue emission at 464 nm involve ¹D₂ as the excited state (transitions ¹D₂ → ³H₆ and ¹D₂ → ³F₄). The excitation of such a high energy state is rare in crystalline hosts [31].

The downconversion emission seen with an excitation by 266 nm radiation and the UC emission excited by 976 nm show a large difference between the intensities of the observed bands particularly for the NIR emission between 760 and 850 nm. 266 nm excitation causes Tm³⁺ ions to populate the ³P multiplet from which ¹G₄ derives population. Multiphonon relaxation to the ¹G₄ state is very unlikely and the population in ³H₄ state remains small and the intensity of the ³H₄ → ³H₆ transition remains small [32].

4 Chromaticity (CIE)

Most lighting specifications nowadays refer to color in terms of the 1931 CIE (Commission Internationale de L'Eclairage) chromatic color coordinates [33] based on the three basic properties of hue, saturation and brightness. Brightness is characterized by a parameter ‘Y’ defined as light intensity factored by the sensitivity of the normal human eye. The chromaticity coordinates ‘x’ and ‘y’ map the color with respect to hue and saturation on a two dimensional CIE chromaticity diagram. The chromaticity coordinates (x, y) can be calculated from the tristimulus value as follows:

$$x = \frac{X}{X + Y + Z}$$

$$y = \frac{Y}{X + Y + Z}$$

The result of this transformation is to factor out the brightness of the color.

Here,

$$X = \int \bar{x}(\lambda)s(\lambda)d\lambda$$

$$Y = \int \bar{y}(\lambda)s(\lambda)d\lambda$$

$$Z = \int \bar{z}(\lambda)s(\lambda)d\lambda$$

Fig. 8 Energy level scheme of Tm^{3+} and Yb^{3+} and proposed up and downconversion mechanism responsible for emissions on 976 nm and 266 nm excitations, respectively

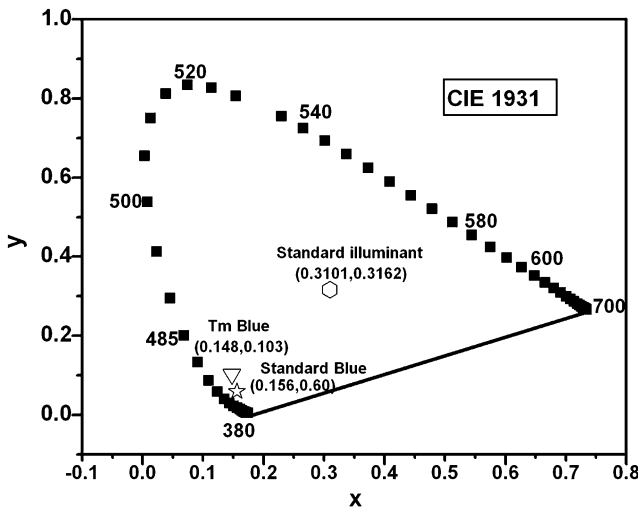
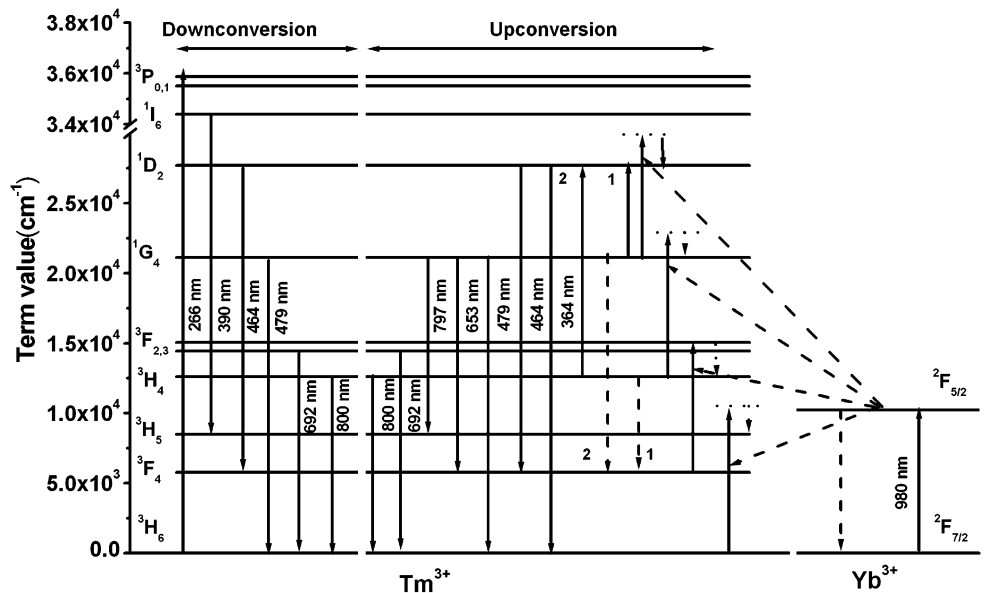


Fig. 9 CIE 1931 chromaticity diagram for blue color. There is a close matching between the standard color coordinate for blue color and the coordinates obtained for blue emission in our experiment

where $\bar{x}(\lambda)$, $\bar{y}(\lambda)$, and $\bar{z}(\lambda)$ are 1931 CIE x , y , and z color matching functions, respectively. $s(\lambda)$ is the spectrum of a light source.

$$\text{Color Purity} = \frac{\sqrt{(x - x_i)^2 + (y - y_i)^2}}{\sqrt{(x_d - x_i)^2 + (y_d - y_i)^2}} \times 100\%$$

where (x, y) and (x_i, y_i) are the color coordinates of the light source and the CIE illuminant, respectively, and (x_d, y_d) is the color coordinate of the dominant wavelength λ_d . The chromatic coordinates, dominant wavelength and color purity compared to the 1931 CIE Standard Source C (illuminant $C = (0.3101, 0.3162)$) for strontium aluminate phosphor were determined from the emission spectrum. The

location of the color coordinates of the three phosphors on the 1931 CIE chromatic diagram is presented in Fig. 9.

The blue emission of the $\text{Tm}^{3+}/\text{Yb}^{3+}$ co-doped phosphor has the CIE chromaticity coordinates (0.148, 0.103) with a dominant wavelength of 470 nm and a color purity of 89%. These coordinates of the blue emission are close to those of the currently available commercial blue phosphors $\text{Y}_2\text{O}_3:\text{Tm}$ (0.158, 0.150) [34], $\text{Sr}_2\text{B}_5\text{O}_9\text{Cl}:\text{Tm}$ (0.166, 0.115) [35], but they differ from that of the standard blue phosphor ZnS:Ag powder ($x = 0.156$, $y = 0.060$) with a dominant wavelength of 455 nm and a color purity of 90% [36]. However, there is scope for improvement in the $\text{SrAl}_4\text{O}_7:\text{Tm}^{3+}/\text{Yb}^{3+}$ phosphor and one may expect better results.

5 Conclusions

A nanocrystalline strontium aluminate (SrAl_4O_7) phosphor doped with $\text{Tm}^{3+} + \text{Yb}^{3+}$ capable of undergoing efficient upconversion emission in the visible and UV when excited with 976 nm radiation has been synthesized and studied. Downconversion emission with 266 nm radiation excitation is also observed. The phosphor was prepared by solution combustion method and the samples were later annealed at 800°C and at 1200°C for 10 h. The luminescence was found to be most intense for Tm^{3+} (0.5 mol%) + Yb^{3+} (2.0 mol%) sample annealed at 1200°C when excited with 976 nm diode laser. Various possible excitation pathways for the different observed emissions are suggested. CIE (x, y) coordinates for the blue emission are calculated and it is found that the sample exhibits vivid blue emission with CIE color coordinates and purity comparable to the standard blue phosphors.

The phosphor is in the SrAl₄O₇ phase and the TEM studies show the presence of rod like structures (submicrometer length) in the post-annealed samples.

Acknowledgements Authors are grateful to Department of Science and Technology (DST), New Delhi for financial assistance. Mr. N.K. Giri and Mr. S.K. Singh thankfully acknowledge the Senior Research Fellowship (SRF) from the Council of Scientific and Industrial Research (CSIR), New Delhi, India. We are also grateful to the Alexander Von Humboldt foundation, Germany for providing Nd:YAG laser.

References

- S. Lingdong, Y. Jiang, L. Changhui, L. Chunsheng, Y. Chunhua, J. Lumin. **87–89**, 447 (2000)
- L.P. Wang, G.Y. Hong, Mater. Res. Bull. **35**, 695 (2000)
- T. Igarashi, M. Ihara, T. Kusunoki, K. Ohno, T. Isobe, M. Senna, J. Nanopart. Res. **3**, 51 (2001)
- C.H. Park, S.J. Park, B.U. Yu, H.S. Bae, C.H. Kim, C.H. Pyun, H.G. Yan, J. Mater. Sci. Lett. **19**, 335 (2000)
- H. Natter, R. Hempelmann, Electrochim. Acta **49**, 51 (2003)
- M. Haase, K. Riwoitzki, H. Meyssamy, A. Kornowski, J. Alloys Compd. **303**, 191 (2000)
- Z. Qiu, Y. Zhou, M. Lu, A. Zhang, Q. Ma, Acta. Mater. **55**, 2615 (2007)
- C. Joshi, K. Kumar, S.B. Rai, J. Appl. Phys. **105**, 123103 (2009)
- L. Xu, B. Wei, Z. Zhang, Z. Lü, H. Gao, Y. Zhang, Nanotechnology **17**, 4327 (2006)
- R. Scheps, Prog. Quantum Electron. **20**, 271 (1996)
- S.K. Singh, K. Kumar, S.B. Rai, Sens. Actuators A **149**, 16 (2009)
- J.M. Fitz-Gerald, T.A. Trottier, R.K. Singh, P.H. Holloway, Appl. Phys. Lett. **72**, 1838 (1998)
- Q.Y. Zhang, K. Pita, S. Buddhudu, C.H. Kam, J. Phys. D, Appl. Phys. **35**, 3085 (2002)
- O.M. Ntwaeaborwa, K.T. Hillie, H.C. Swart, Phys. Stat. Sol. (c) **1**, 2366 (2004)
- T. Matsuzawa, Y. Aoki, N. Takeuchi, Y. Murayama, J. Electrochem. Soc. **143**, 2670 (1996)
- F. Vetrone, J.C. Boyer, J.A. Capobianco, A. Speghini, M. Bettinelli, Nanotechnology **15**, 75 (2004)
- F.W. Ostermayer, J.P. Ziel, H.M. Marcos, L.G. Van Uitert, J.E. Geusic, Phys. Rev. B **3**, 2698 (1971)
- T. Katsumata, K. Sasajima, T. Nabae, S. Komuro, T. Morikawa, J. Am. Ceram. Soc. **81**, 413 (1998)
- T. Katsumata, T. Nabae, K. Sasajima, S. Komuro, T. Morikawa, J. Electrochem. Soc. **144**, L243 (1997)
- I.C. Chen, T.M. Chen, J. Mater. Res. **16**, 644 (2001)
- O.A. Tanori, R. Melendrez, M.P. Montero, B. Castaneda, V. Chernov, W.M. Yen, M.B. Flores, J. Lumin. **128**, 173 (2008)
- R.S. Niedbala, H. Feindt, K. Kardos, T. Vail, J. Burton, B. Bielska, S. Li, D. Milunic, P. Bourdelle, R. Vallejo, Anal. Biochem. **293**, 22 (2001)
- E. Downing, L. Hesselink, J. Ralston, R.A. Macfarlane, Science **273**, 1185 (1996)
- S.K. Singh, K. Kumar, S.B. Rai, Appl. Phys. B **94**, 165 (2009)
- S.D. Han, K.C. Singh, T.Y. Cho, H.S. Lee, D. Jakhar, J.P. Hulme, C.H. Han, J.D. Kim, I.S. Chun, J. Gwak, J. Lumin. **128**, 301 (2008)
- P. Zhang, L. Li, M. Xub, L. Liu, J. Alloys Compd. **456**, 216 (2008)
- J. Chen, F. Gu, C. Li, Cryst. Growth Des. **8**, 3175 (2008)
- X. Yuan, Y. Xu, G. Huang, C. Zeng, J. Am. Ceram. Soc. **90**, 2283 (2007)
- Y. Zhu, M. Zheng, J. Zeng, Y. Xiao, Y. Liu, Mater. Chem. Phys. **113**, 721 (2009)
- F. Pandozzi, F. Vetrone, J.C. Boyer, R. Naccache, J.A. Capobianco, A. Speghini, M. Bettinelli, J. Phys. Chem. B **109**, 17400 (2005)
- Y. Guyot, R. Moncorge, L.D. Merkle, A. Pinto, B. McIntosh, H. Verdun, Opt. Mater. **5**, 127 (1996)
- L.A. Riseberg, H.W. Moos, Phys. Rev. **174**, 429 (1968)
- G.B. Stringfellow, M.G. Crawford, *High Brightness Light Emitting Diodes*. Semiconductors and Semimetals, vol. 48 (Academic Press, San Diego, 1997), p. 247
- J. Hao, S.A. Studenikin, M. Cocivera, J. Lumin. **93**, 313 (2001)
- J. Hao, M. Cocivera, J. Phys., Condens. Matter. **14**, 925 (2002)
- R.Y. Lee, F.L. Zhang, J. Penczek, B.K. Wagner, P.N. Yocom, C.J. Summers, J. Vac. Sci. Technol. B **16**, 855 (1998)